

# Alzheimer-Like Changes in Rat Models of Spontaneous Diabetes

Zhen-guo Li,<sup>1</sup> Weixian Zhang,<sup>1</sup> and Anders A.F. Sima<sup>1,2</sup>

**OBJECTIVE**—To examine whether changes characteristic of Alzheimer's disease occur in two rat models with spontaneous onset of type 1 and type 2 diabetes.

**RESEARCH DESIGN AND METHODS**—The frontal cortices of 8-month-diabetic rats were examined with respect to neuronal densities, neurite degeneration, expression, and/or immunolocalization of amyloid precursor protein (APP),  $\beta$ -secretase,  $\beta$ -amyloid, COOH-terminal fragment (CTF), insulin receptor, IGF-1 receptor, glycogen synthase kinase 3- $\beta$  (GSK-3 $\beta$ ), protein kinase B (Akt), phosphorylated  $\tau$  (phospho- $\tau$ ), synaptophysin, and phosphorylated neurofilaments (SMI-31).

**RESULTS**—Neuronal loss occurred in both models, significantly more so in type 2 diabetic BBZDR/Wor rats compared with type 1 diabetic BB/Wor rats and was associated with a ninefold increase of dystrophic neurites. APP,  $\beta$ -secretase,  $\beta$ -amyloid, and CTF were significantly increased in type 2 diabetic rats, as was phospho- $\tau$ . The insulin receptor expression was decreased in type 1 diabetes, whereas IGF-1 receptor was decreased in both models, as were Akt and GSK-3 $\beta$  expression.

**CONCLUSIONS**—The data show that  $\beta$ -amyloid and phospho- $\tau$  accumulation occur in experimental diabetes and that this is associated with neurite degeneration and neuronal loss. The changes were more severe in the type 2 diabetic model and appear to be associated with insulin resistance and possibly hypercholesterolemia. The two models will provide useful tools to unravel further mechanistic associations between diabetes and Alzheimer's disease. *Diabetes* 56:1817–1824, 2007

Cognitive impairments are more common in diabetic patients than in nondiabetic subjects (1–3), which in part is due to ischemic events resulting from cerebral micro- and/or macrovascular disease or to repeated episodes of severe hypoglycemia. These conditions have been referred to as “secondary diabetic encephalopathy” (4). However, during the last decade there is accumulating evidence suggesting that cognitive dysfunction is also caused by diabetic

dysmetabolism, so-called “primary diabetic encephalopathy” (1–4).

This appears to be true also in experimental models of diabetes. In the streptozotocin-induced diabetic rat, impaired cognitive performances have been associated with impaired hippocampal plasticity, changes that are reversed by insulin treatment (5). In type 1 diabetic BB/Wor rats, progressively impaired cognitive function is associated with suppressed insulin and IGF-1 actions and neuronal apoptosis in hippocampus (6), changes that are significantly prevented by insulinomimetic C-peptide (7). Taken together these data suggest mechanistic links between impaired insulin- and IGF-1-signaling in diabetes and cognitive dysfunction.

Hyperglycemia, perturbed function of insulin, and IGF-1 signaling have been proposed as pathogenetic factors contributing to Alzheimer's disease (8–10), suggesting that diabetes and Alzheimer's disease may share common underlying causative mechanisms. Insulin and IGF-1 levels are decreased in the brains of patients with Alzheimer's disease due to impaired transport across the blood-brain barrier (11), and the cerebral cellular sensitivities to these factors are attenuated (12–14). Apart from several mutations that have been identified and linked to the pathophysiology in a small percentage of Alzheimer's disease cases (15,16), other factors invoked in the pathogenesis of sporadic Alzheimer's disease include vascular dysfunction, accumulation of free radicals, immune dysfunction, and hypercholesterolemia (17–18). Alzheimer's disease is characterized by abnormal accumulation of extra- and intracellular  $\beta$ -amyloid with formation of extracellular senile plaques and intracellular cytotoxic effects, respectively (19–20). The second cardinal pathology characteristic of Alzheimer's disease is abnormal cleavage and hyperphosphorylation of the microtubule-associated  $\tau$  protein, resulting in neurofibrillary tangles and neurite degeneration (21,22).

To explore possible underlying linkages between long-standing diabetes and Alzheimer's disease under experimental conditions, we examined abnormalities in insulin signaling and amyloid precursor protein (APP) metabolism, hyperphosphorylation of  $\tau$ , neuronal loss, and neurite degeneration in two rat models with spontaneous onset of diabetes. They are outbred on the same genetic background: the type 1 diabetic BB/Wor-rat and the type 2 diabetic BBZDR/Wor-rat. Both models develop diabetes around 75 days of age and are maintained at the same level of hyperglycemia (23). The type 1 BB/Wor-rat develops insulinopenic diabetes secondary to an immune-mediated destruction of pancreatic  $\beta$ -cells and hence requires daily insulin supplementation. In the type 2 BBZDR/Wor-rat, the onset of diabetes is preceded by obesity and it develops

From the <sup>1</sup>Department of Pathology, Wayne State University, School of Medicine, Detroit, Michigan; and the <sup>2</sup>Department of Neurology, Wayne State University, School of Medicine, Detroit, Michigan.

Address correspondence and reprint requests to Dr. Anders A.F. Sima, Department of Pathology, Wayne State University, School of Medicine, 540 E. Canfield Ave., Detroit, MI 48201. E-mail: asima@med.wayne.edu.

Received for publication 6 February 2007 and accepted in revised form 12 April 2007.

Published ahead of print at <http://diabetes.diabetesjournals.org> on 24 April 2007. DOI: 10.2337/db07-0171.

APP, amyloid precursor protein; CNS, central nervous system; CTF, COOH-terminal fragment; GFAP, glial fibrillary acid protein; GSK-3 $\beta$ , glycogen synthase kinase 3- $\beta$ .

© 2007 by the American Diabetes Association.

The costs of publication of this article were defrayed in part by the payment of page charges. This article must therefore be hereby marked “advertisement” in accordance with 18 U.S.C. Section 1734 solely to indicate this fact.

peripheral insulin resistance with hyperinsulinemia accompanied by hypercholesterolemia and hyperlipidemia. However, as to whether resistance to insulin action occurs in the central nervous system (CNS) of the latter model is not known. Hence, these two models replicate closely the two major types of human diabetes (23,24).

## RESEARCH DESIGN AND METHODS

Prediabetic male type 1 BB/Wor ( $n = 10$ ) and type 2 BBZDR/Wor rats ( $n = 10$ ) and sex- and age-matched non-diabetes-prone BB-control rats ( $n = 10$ ) were obtained from Biomedical Research Models (Worcester, MA). All diabetic animals were maintained in metabolic cages and cared for in accordance with the guidelines of the Wayne State University Animal Investigation Committee and those of the National Institutes of Health (publication #85-23, 1995). Urine volume and glucose levels were measured daily to ascertain the onset of diabetes and to titrate daily insulin doses for type 1 BB/Wor rats. Blood glucose levels were measured weekly using blood glucose test strips (Bayer, Mishawaka, IN). Diabetes developed spontaneously in BB/Wor rats at  $73 \pm 2$  days of age and in BBZDR/Wor rats at  $76 \pm 4$  days. Type 1 diabetic rats were treated with daily titrated doses (0.5–3.0 IU) of protamine zinc insulin (Blue Ridge Pharmaceuticals, Greensboro, NC) to maintain blood glucose levels between 20 and 25 mmol/l and to prevent ketoacidosis (10). At the time of death (18 h after last insulin injection of type 1 diabetic rats), serum insulin and IGF-1 concentrations were analyzed using radioimmunoassay kits (Linco Research, St. Charles, MO), GHb was measured using a DCA 2000 Analyzer (Bayer, Elkhart, IN). Cholesterol levels were obtained (Biomedical Research Models, Worcester, MA). Both type 1 diabetic BB/Wor and type 2 diabetic BBZDR/Wor rats were killed after 8 months of diabetes, i.e., ~10.5 months of age.

**Tissue collection.** Four animals per group were prepared for cortical neuronal counts and immunocytochemical studies. Rats were anesthetized with an intraperitoneal overdose of sodium pentobarbital (120 mg/kg body wt). Each rat was perfused transcardially through the left ventricle with 300 ml PBS (pH 7.4), followed by 4% paraformaldehyde in PBS (pH 7.4). After perfusion, the whole brain was dissected and placed in the same fixative overnight.

For protein isolation, six animals per group were used. The animals were anesthetized with isoflurane and decapitated. The brains were rapidly removed and placed on an ice-cooled cutting board. The meninges were removed and the hemispheres separated. The bilateral frontal cortices between Bregma 5.2 and 3.2 mm (25) were dissected coronally, snap frozen in liquid nitrogen, and stored at  $-70^{\circ}\text{C}$ .

**Assessment of neuronal density.** Coronal segments of the frontal cortex between Bregma 5.2 and 3.2 mm were embedded in paraffin. Ten 6- $\mu\text{m}$ -thick paraffin sections 90  $\mu\text{m}$  apart were deparaffinized, rehydrated in distilled water, and stained with FD cresyl violet solution (FD Neuro Technologies, Baltimore, MD). After washing in distilled water three times, sections were differentiated in 95% ethanol containing 0.1% glacial acetic acid for 1 min and dehydrated in 100% ethanol followed by clearing in xylene. Images of perpendicularly sectioned cortex of ~1.5 mm in length were captured and analyzed using an Image-Pro Plus 3.0 image analysis software (Media Cybernetics, Silver Spring, MD). The cortex was separated into layers I, II–III, IV, V, VIa, and VIb (25). Only neurons displaying visible nuclei were counted, and their numbers in each layer were expressed per area unit ( $n$  per millimeters squared).

**Immunocytochemistry.** Deparaffinized 6- $\mu\text{m}$  sections of the frontal cortex were incubated with the primary antibody for 30 min at room temperature, washed with three changes of PBS, and incubated with the peroxidase-conjugated secondary antibody (Vector Lab., Burlingame, CA) for 30 min at room temperature. The immunoreactive products were visualized with diaminobenzidine as color chromogen. Counterstaining was performed with hematoxylin to show nuclear staining. Primary antibodies used were: mouse anti-BACE1 antibody (Chemicon, Temecula, CA), rabbit anti- $\beta$ -APP antibody (Zymed Lab., South San Francisco, CA), mouse anti-sAPP (A4, aa 68–81 of APP; Chemicon), rabbit anti-COOH-terminal fragment (CTF) (C-term 751-770; Calbiochem, LaJolla, CA), rabbit anti-phospho-Akt (Thr308) and anti-phospho-glycogen synthase kinase 3- $\beta$  (GSK-3 $\beta$ ) (Ser9) antibodies (Cell Signaling, Danvers, MA), mouse anti-synaptophysin and rabbit anti-glial fibrillary acid protein (GFAP) antibodies (Sigma-Aldrich, St. Louis, MO), monoclonal mouse anti-phosphorylated neurofilament M and neurofilament N (SMI-31; Covance, Berkeley, CA), rabbit anti-IGF-I receptor and insulin receptor  $\beta$ -subunit (IR $\beta$ ) antibodies (Santa Cruz Biotechnology, Santa Cruz, CA), monoclonal mouse anti- $\beta$ -amyloid antibody 4G8 (against  $\beta$ -amyloid aa 18–22[VFFAE]; Conva- nce), and rabbit anti-phospho  $\tau$  (phospho- $\tau$ ) antibody (PS396) (gift from Dr. Koichi Ishiguro, Mitsubishi Kagaku Institute of Life Sciences, Tokyo, Japan).

Additional immunofluorescence staining was used for synaptophysin. Sections were deparaffinized, rehydrated, and blocked with PBS containing 10% goat serum at room temperature for 30 min and incubated with the primary antibody for 1 h. After washing three times with PBS, sections were incubated with the Alexa Fluor 499 goat anti-mouse IgG (Invitrogen, Carlsbad, CA) as secondary antibody. The fluorescent immunoreactive products were visualized under a Leica DMLB microscope (Leica Microsystems Wetzlar, Wetzlar, Germany).

Negative controls were performed by omitting the primary antibody. To further ensure specific labeling, secondary antibodies (6  $\mu\text{l/ml}$ ) of anti-mouse IgG or anti-rabbit IgG were incubated with 4% normal rat serum in room temperature for 30 min and then applied to the tissue slides (26). Comparisons with nonpreabsorbed secondary antibodies revealed the same results (data not shown). In a second set of control experiments, isotype experiments were performed in which the primary monoclonal antibodies (IgG $_1$  and IgG $_{2b}$ ), were replaced by nonimmune IgG $_1$  and IgG $_{2b}$  control immunoglobulins (Santa Cruz Biotechnology) (27). Tissue slides treated accordingly showed no immunoreactivity (data not shown).

**Quantitative analyses of synaptophysin, dystrophic neuritis, and gliosis.** Cortical sections immunostained with synaptophysin were examined densitometrically. The intensity range of immunostaining was assessed by a gray scale paradigm using Image-Pro image analysis (Media Cybernetics). Four randomly chosen areas of cortical layers II–III from each of 10 sections from three animals per group were examined. Sections immunostained with SMI-31 were used to examine the density of dystrophic neurites. Eight areas (each measuring 0.284 mm $^2$ ) chosen as above were assessed in each of three animals. The number of dystrophic neurites per area was calculated and expressed as number per millimeters squared. The density of GFAP-positive astrocyte somata was calculated in the same fashion and expressed as number per millimeters squared.

**Immunoblotting.** Dissected frontal cortices between Bregma 5.2 and 3.2 mm from six animals were used. Protein lysates (40  $\mu\text{g/lane}$ ) were resolved by SDS-PAGE electrophoresis under reducing conditions and transferred to polyvinylidene difluoride membranes (Millipore, Bedford, MA) or nitrocellulose membranes (Bio-Rad, Hercules, CA). Membranes were stained with 1% Ponceau S or the expression of actin was used to ensure equal loading. The membranes were blocked with 5% BSA in Tris-buffered saline with Tween (TBST) at room temperature for 1 h and incubated with the primary antibody in the blocking solution for 1 h at room temperature. The antibodies used were the same as those used for immunocytochemistry. The blots were washed three times with TBST and incubated for 1 h with the horseradish peroxidase-conjugated secondary antibody (Santa Cruz Biotechnology), followed by an enhanced chemiluminescence detection system (Amersham Pharmacia Biotech, Piscataway, NJ) and exposed to Kodak X-OMAT blue film (Eastman Kodak, Rochester, NY). The immunoblots were quantitated using Scion Image analysis software (Scion, Frederick, MD).

**Statistical methods.** All data are reported as means  $\pm$  SD. Comparisons were made using ANOVA. When a  $P < 0.05$  was obtained, group comparisons were made using Scheffes post hoc test. Significance was defined as a  $P$  value  $< 0.05$ . All analyses were performed by personnel being unaware of the animal identities.

## RESULTS

**Clinical observations.** After 8 months of diabetes, type 2 diabetic BBZDR/Wor rats were 24% heavier ( $P < 0.05$ ) than control rats, whereas the weight of type 1 diabetic BB/Wor rats was 77% ( $P < 0.001$ ) of that of control animals. Both type 1 and type 2 diabetic rats showed significantly ( $P < 0.001$ ) elevated blood glucose levels and GHb values with no differences between the two diabetic models (Table 1). Plasma insulin levels were markedly decreased in type 1 ( $P < 0.001$ ) and elevated ( $P < 0.05$ ) in type 2 diabetic rats. Plasma IGF levels were significantly and similarly decreased ( $P < 0.001$ ) in both models. Cholesterol levels were elevated in type 2 diabetic BBZDR/Wor rats ( $P < 0.001$ ) but not in their type 1 counterparts. **Neuronal densities in frontal cortex.** Cell counts of neuronal populations in layers I–VIb of the frontal cortex showed significantly decreased densities in all layers in type 2 diabetic BBZDR/Wor rats ( $P < 0.05$  or less), being most severe in layers II–III and IV ( $P < 0.005$ ) (Fig. 1A), in which the densities were decreased by 40–50%. The neuronal loss in these layers was significantly less ( $P < 0.005$

TABLE 1

Body weight, plasma glucose, GHb, insulin, IGF-1, and cholesterol levels in control, type 1 BB/Wor, and type 2 BBZDR/Wor rats at 8 months of diabetes

	<i>n</i>	Body wt (g)	Plasma glucose (mmol/dl)	GHb (%)	Plasma insulin (pmol/l)	Plasma IGF-1 (ng/ml)	Cholesterol (mg/dl)
Control rats	10	502.3 ± 12.2	5.1 ± 0.3	3.1 ± 0.2	457 ± 17	1,181 ± 29	135 ± 31
Type 1 diabetic BB/Wor rats	10	385.3 ± 7.6***†	24.9 ± 2.7**	11.4 ± 0.6**	51 ± 6**	776 ± 75**	147 ± 45†
Type 2 diabetic BBZDR/Wor rats	10	622.6 ± 157.3*	23.9 ± 4.6**	11.7 ± 0.7**	568 ± 56*	887 ± 85**	315 ± 36**

Data are means ± SD. \* $P < 0.05$ , \*\* $P < 0.001$  vs. control rats; † $P < 0.001$  vs. BBZDR/Wor rats.

and  $P < 0.01$ , respectively) in type 1 diabetic BB/Wor rats, although these animals also demonstrated significant losses ( $P < 0.05$  or less) in all layers except for layer I (Fig. 1A). The neuronal loss was accompanied by a noticeable astrogliosis as illustrated by GFAP-positive astrocytes. Astrocyte density was increased sixfold in BBZDR/Wor rats ( $P < 0.001$ ), which was significantly ( $P < 0.001$ ) greater than the 3.7-fold increase ( $P < 0.01$ ) in BB/Wor rats (Fig. 1B). Densitometric evaluation of synaptophysin positivity, reflecting synapse density, was decreased by ~35% in both type 1 and type 2 diabetic rats (both  $P < 0.001$ ) (Fig. 1C). Degenerated dystrophic neurites visualized by immunostaining for phosphorylated neurofilaments (Fig. 1D) were increased 8.6-fold ( $P < 0.001$ ) in BBZDR/Wor rats, which was significantly ( $P < 0.001$ ) greater than the 2.7-fold increase ( $P < 0.01$ ) in BB/Wor rats (Fig. 1D). Dystrophic neurites occasionally occurred in clusters (Fig. 1E), which were not associated with extracellular deposits of  $\beta$ -amyloid, or as single dystrophic neurites (Fig. 1F).

**APP,  $\beta$ -secretase,  $\beta$ -amyloid, soluble APP, and CTF expression and localization in frontal cortex.** The protein expression of APP,  $\beta$ -secretase, and  $\beta$ -amyloid was increased in diabetic rats compared with age-matched control rats (Fig. 2A–C). These upregulations were significantly ( $P < 0.05$  or less) more pronounced in type 2 diabetic BBZDR/Wor-rats than in the type 1 diabetic BB/Wor counterparts. The more than twofold increases in the expression of these proteins in BBZDR/Wor rats corresponded immunocytochemically to a more intense staining of APP,  $\beta$ -secretase, and  $\beta$ -amyloid in frontal cortical neurons compared with control rats (Fig. 3A–C). To maximize the capture of  $\beta$ -amyloid, nitrocellulose membranes (0.2  $\mu$ m) were used and protein lysates were boiled before loading. However, monomeric  $\beta$ -amyloid (4 kd) could not be detected. Instead, the multimeric form of  $\beta$ -amyloid was detected between 6.5 and 1.0 kd (Fig. 2C). In type 2 diabetic rats, most neurons showed intense APP staining, whereas control rats showed less intense staining. The staining pattern in type 1 diabetic rats was intermediate between that of type 2 diabetic and control rats. Similar differences between the three groups of animals were displayed by positive  $\beta$ -secretase staining (Fig. 3B). APP and  $\beta$ -secretase often showed a punctate positive staining of the neurolemma (Fig. 3A, B, and D).  $\beta$ -Amyloid-positive staining was weak in the cytoplasm of control neurons, a staining pattern that was increased in type 1 and more so in type 2 diabetic rats (Fig. 3C). In none of the animals could extracellular deposits of  $\beta$ -amyloid be demonstrated. The expressions of soluble APP (Fig. 2D) and CTF (Fig. 2E) were minimally increased in type 1 diabetic BB/Wor rats but showed a more than twofold

increase ( $P < 0.01$  and  $P < 0.005$ , respectively) in type 2 BBZDR/Wor rats.

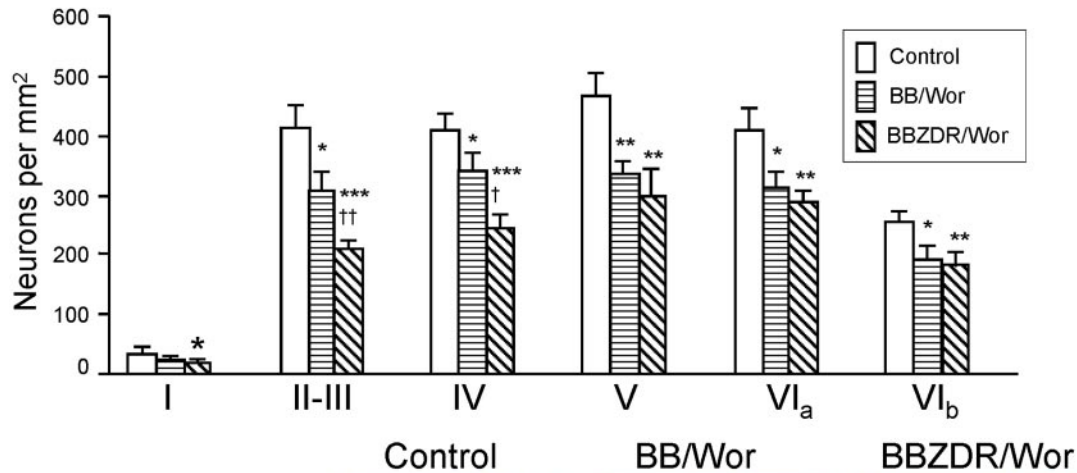
**Expression and localization of phospho- $\tau$  protein.** Western blotting for phospho- $\tau$  demonstrated several bands corresponding to the multiple phospho- $\tau$  isoforms (Fig. 4A). Phospho- $\tau$  was significantly more expressed in type 2 diabetic BBZDR/Wor rats than in control ( $P < 0.01$ ) and BB/Wor rats ( $P < 0.05$ ) (Fig. 4A), which corresponded to a more intense immunostaining of phospho- $\tau$  in cortical neurons in type 2 diabetic rats (Fig. 4B) associated with a punctate staining pattern in the neuropil. The neuronal staining pattern was less evident in type 1 diabetic rats in whom the expression of phospho- $\tau$  was not significantly increased. Only faint positivity was evident in age-matched control rats (Fig. 4B). Intracytoplasmic phospho- $\tau$ -positive tangle-like inclusions were not observed.

**Abnormalities of the insulin signaling pathway.** The expression of the insulin receptor  $\beta$ -subunit was significantly ( $P < 0.01$ ) decreased in the frontal cortex of type 1 diabetic BB/Wor but not in type 2 diabetic BBZDR/Wor rats (Fig. 5A). On the other hand, the expression of the IGF-1 receptor  $\beta$ -subunit was equally suppressed in type 1 and type 2 diabetic rats ( $P < 0.05$ ) (Fig. 5B). In the insulin signaling pathway, phosphorylation of protein kinase B (Akt) is important for GSK-3 $\beta$  (Ser 9) phosphorylation, which suppresses GSK-3 $\beta$ , an important phosphokinase implicated in  $\tau$  phosphorylation (28). In the present study, the expression of phosphorylated Akt was significantly ( $P < 0.01$ ) decreased in frontal cortex of both type 1 and type 2 diabetic rats (Fig. 5C), which was accompanied by an ~50% reduction ( $P < 0.05$ ) in phosphorylated GSK-3 $\beta$  (Ser 9) expression in both diabetic models (Fig. 5D). These findings are in keeping with the notion that disinhibition of phosphorylated GSK-3 $\beta$  by GSK-3 $\beta$  (Ser 9) is in part responsible for  $\tau$  phosphorylation (28).

## DISCUSSION

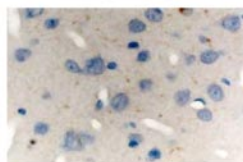
Alzheimer's disease is characterized by an increased  $\beta$ -amyloid load, accumulation of hyperphosphorylated  $\tau$ , neurite degeneration, and neuronal loss (19,21,22). In this study, we demonstrate significant loss of frontal cortical neurons and neurite degeneration in chronically diabetic rats, accompanied by increased expression of APP, its cleavage enzyme  $\beta$ -secretase, and increased sAPP and  $\beta$ -amyloid burden as well as CTR, abnormalities that were more expressed in type 2 diabetic BBZDR/Wor rats. Phosphorylation of cleaved  $\tau$  was markedly increased in type 2 diabetic rats. In this model, phospho- $\tau$  was associated with suppressed expression of insulin signaling intermediaries, despite the fact that the insulin receptor expression

## A Neuronal densities in frontal cortex

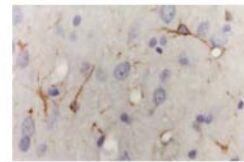


## B GFAP

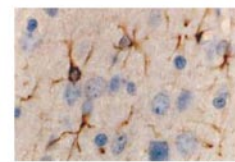
Density of positive glial cells (per mm<sup>2</sup>)



83 ± 18



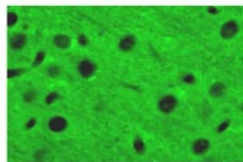
305 ± 41\*\*



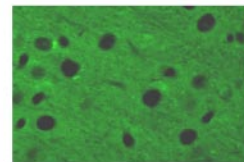
551 ± 45 \*\*\*\* ††

## C Synaptophysin

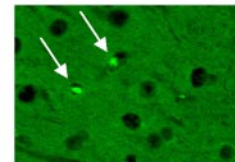
Relative staining intensity



2.05 ± 0.1



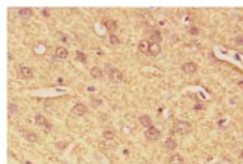
1.30 ± 0.06 \*\*\*\*



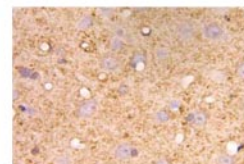
1.27 ± 0.05 \*\*\*\*

## D SMI-31

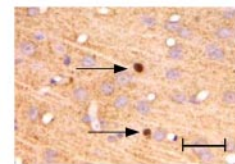
Density of dystrophic neurites (per mm<sup>2</sup>)



74 ± 9



198 ± 37\*\*



635 ± 57 \*\*\*\* †††

## E

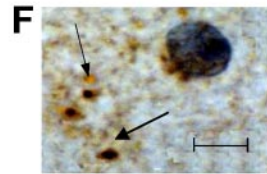
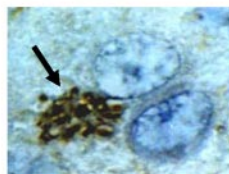


**FIG. 1.** Quantitative assessment of neuronal densities in frontal cortical layers I–VIb (A). Both type 1 BB/Wor and type 2 BBZDR/Wor rats showed significantly decreased neuronal densities, being significantly more severe in layers II–III and IV in type 2 diabetic rats. The neuronal loss was accompanied by GFAP-positive astrogliosis in layers II–III (B) and a lesser density of synaptophysin-positive staining in the neuropil in diabetic rats. In type 2 diabetic rats, enlarged synapses were occasionally demonstrated (arrows in C). Immunostaining for phosphorylated

filaments (SMI-31) demonstrated occasional dystrophic neurites in type 2 diabetic rats (arrows in D). These occurred occasionally as clusters of expanded neurites (thick arrow in E) or as single expanded neurites (thin arrows in F). The densities of SMI-31-positive neurites were increased in diabetic rats. All micrographs are from layers II–III. The bar in Fig. 1D corresponds to 50 μm and is representative of Fig. 1B–D. The bar in Fig. 1F corresponds to 12.5 μm and is the same for Fig. 1E. \**P* < 0.05, \*\**P* < 0.01, \*\*\**P* < 0.005, \*\*\*\**P* < 0.001 vs. control rats; †*P* < 0.01, ††*P* < 0.005, †††*P* < 0.001 vs. BB/Wor rats.

was unaltered, although that of the IGF-1 receptor was downregulated. This constellation may reflect increased caveolin-1 activity in cholesterol-rich lipid rafts that enhances the expression of insulin receptor, whereas other growth factor receptors, including that of IGF-1, are suppressed (29,30). The more severe neurite degenerative changes in the type 2 diabetic BBZDR/Wor rat is in keeping with the toxic effects of altered β-amyloid and phospho-τ in this model. These findings indicate that experimental diabetes, particularly type 2 diabetes, develops abnormalities that characterize early Alzheimer's disease.

The differences in the severity between the two types of

diabetes cannot be related to differences in hyperglycemic exposures, since these were the same in the two models. In the type 2 diabetic rats, the insulin receptor expression was normal, despite that they demonstrated impaired insulin signaling activities, indicating that the CNS also develops insulin resistance downstream from the receptor and hence impaired insulin signaling and action, as do peripheral tissues in this model (24). This is the first evidence demonstrating perturbed CNS insulin signaling in type 2 experimental diabetes, although diet-induced insulin resistance in the CNS has been shown in transgenic Tg 2576 mice, which model Alzheimer's disease (31). Impaired

## Immunoblots

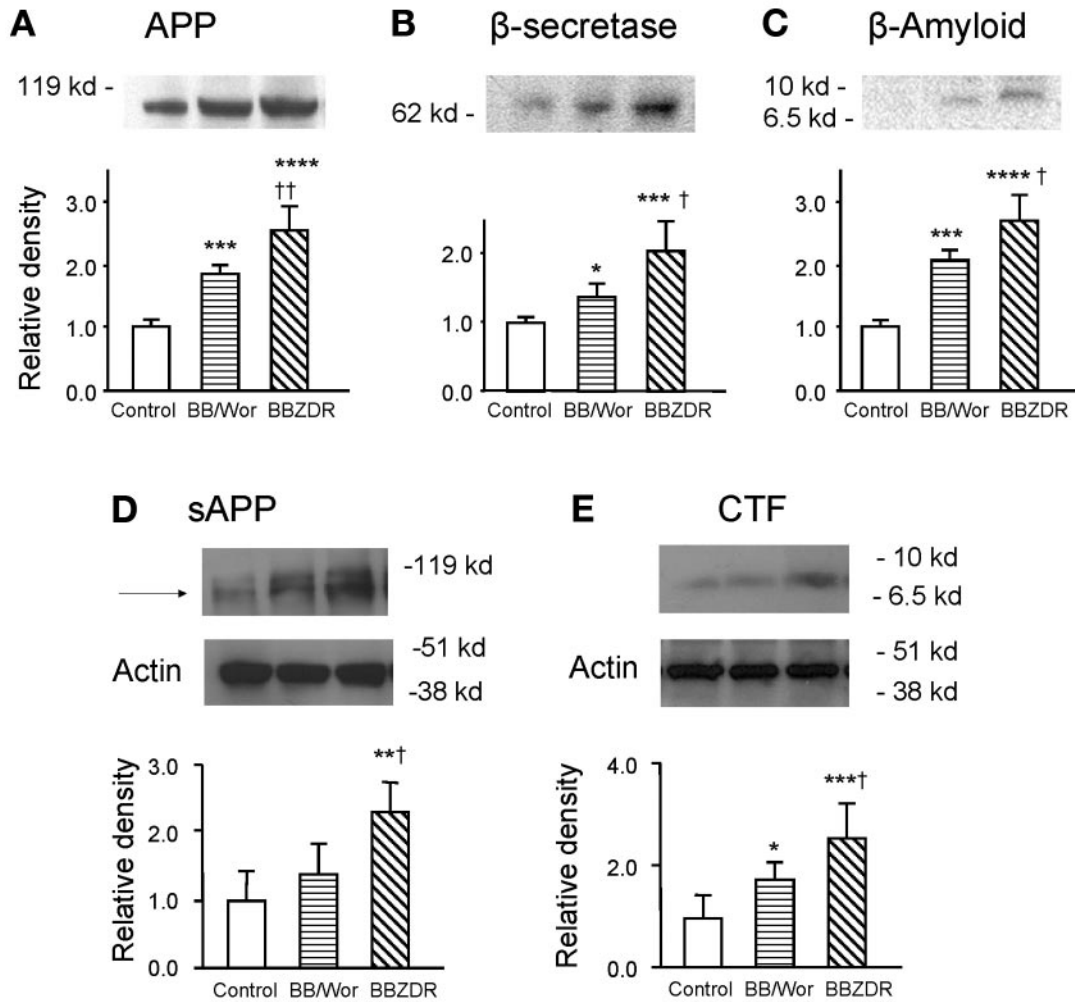


**FIG. 2.** Immunoblotting of APP (A),  $\beta$ -secretase (B), and  $\beta$ -amyloid (C) from frontal cortices in control and type 1 and type 2 diabetic rats. Note increased expression of APP,  $\beta$ -secretase, and  $\beta$ -amyloid in both diabetic animals and significantly greater increases in type 2 diabetic rats. The expression of  $\beta$ -amyloid represents the multimeric form of  $\beta$ -amyloid (between 6.5 and 10 kd). The expression of sAPP and CTF was only mildly increased in type 1 BB/Wor rats (D and E), whereas type 2 BBZDR/Wor rats showed a more than twofold increase in the expression of sAPP and CTF (D and E). \* $P < 0.05$ , \*\* $P < 0.01$ , \*\*\* $P < 0.005$ , \*\*\*\* $P < 0.001$  vs. control rats; † $P < 0.05$ , †† $P < 0.01$  vs. BB/Wor rats.

insulin signaling has also been described in hippocampus after intraventricular injection of streptozotocin (32). Similar abnormalities in insulin signaling intermediaries in type 1 diabetic rats are probably related primarily to suppressed expression of the insulin receptor itself and hence different from the insulin resistance in type 2 diabetic animals. The differences between the two models are similar to those previously demonstrated in hippocampus (33). Despite the fact that insulin signaling appeared to be affected to similar extents in the two models, although for different reasons, the phospho- $\tau$  abnormalities were significantly more expressed in the type 2 model, suggesting that additional factors must be considered. Other so-called " $\tau$ -kinases" include cyclin-dependent kinases (cdk 5), mitogen-activated protein kinase family members, extracellular regulated kinase 1/2, and p38 and c-jun NH<sub>2</sub>-terminal kinase (34). The negative regulation of  $\tau$  phosphorylation by O-GlcNAcylation due to deficient brain glucose uptake has been invoked in Alzheimer's disease (35). A similar "yin-yang" relationship between O-GlcNAc and phosphorylation exists with respect to nodal ankyrin<sub>G</sub> in diabetic rats (36). Since the expression of the IGF-1 receptor,

another factor implicated in the pathogenesis of Alzheimer's disease (12), was affected equally in the two models, this is not likely to account for the discrepancies in the expression of Alzheimer's disease-like changes.

Both clinical and experimental studies suggest that overweight is a contributing risk factor in Alzheimer's disease. This linkage is believed to be mediated by insulin resistance and/or dysfunction of the hypothalamic-pituitary-adrenal axis (31,37,38). Although corticosterone measurements were not performed in this study, the type 2 diabetic BBZDR/Wor rats examined here were obese and insulin resistant. Conversely, caloric restriction and leaner body weight, as in the BB/Wor rats, have a protective effect on Alzheimer's disease-like changes in transgenic mouse models (39,40). Therefore, differences in body weight between the two models used here could contribute to the differences in the expression of Alzheimer's disease-like changes.

Hypercholesterolemia has been associated with Alzheimer's disease with formation of caveolae and lipid rafts, invaginations of plasma membranes enriched in cholesterol and sphingolipids (41). Cholesterol levels were significantly elevated in type 2 but not in type 1 diabetic rats.

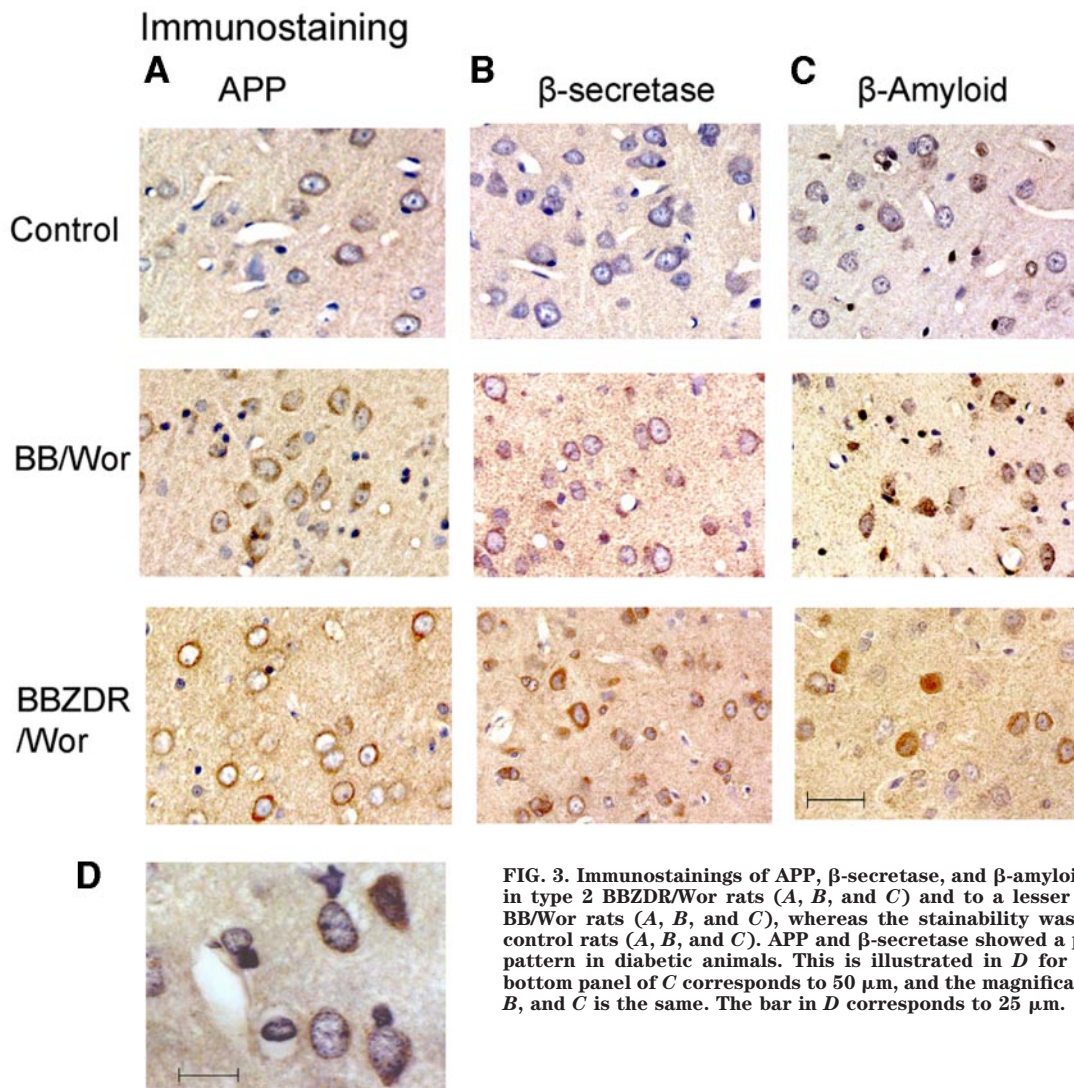


FIG. 3. Immunostainings of APP,  $\beta$ -secretase, and  $\beta$ -amyloid were increased in type 2 BBZDR/Wor rats (A, B, and C) and to a lesser extent in type 1 BB/Wor rats (A, B, and C), whereas the stainability was least evident in control rats (A, B, and C). APP and  $\beta$ -secretase showed a punctate staining pattern in diabetic animals. This is illustrated in D for APP. The bar in bottom panel of C corresponds to 50  $\mu$ m, and the magnification for panels A, B, and C is the same. The bar in D corresponds to 25  $\mu$ m.

Associated caveolin signaling has been postulated to influence the activity of several growth factor receptors including those of insulin and IGF-1 (42). Furthermore, the formation of lipid rafts are coupled with upregulation of APP and  $\beta$ -secretase (43,44). The punctate stainability of APP and  $\beta$ -amyloid on the neurolemma as demonstrated here could potentially represent their concentration to caveolae. APP is also upregulated by hyperglycemia under hypoxic conditions (9) and by perturbed insulin signaling (13). Cholesterol loading enhances  $\beta$ - and  $\gamma$ -secretase activities, which result in enhanced release of amyloidogenic  $\beta$ -amyloid (44), as  $\beta$ -amyloid is generated by the sequential cleavage of APP by  $\beta$ - and  $\gamma$ -secretase.

Therefore, hypercholesterolemia, present only in type 2 diabetic BBZDR/Wor rats, may in part, through formation of caveolae and lipid rafts, explain the unaltered expression of the insulin receptor and the downregulation of the IGF-1 receptor via caveolin action as well as the significantly greater upregulation of APP and  $\beta$ -secretase, resulting in a greater  $\beta$ -amyloid burden in the type 2 diabetic animals. Despite the fact that  $\beta$ -amyloid was markedly increased in BBZDR/Wor rats, no extracellular deposits of  $\beta$ -amyloid could be detected. It has been demonstrated that Wortmannin, which blocks insulin signaling, hampers the release of soluble APP and  $\beta$ -amyloid from the intra-

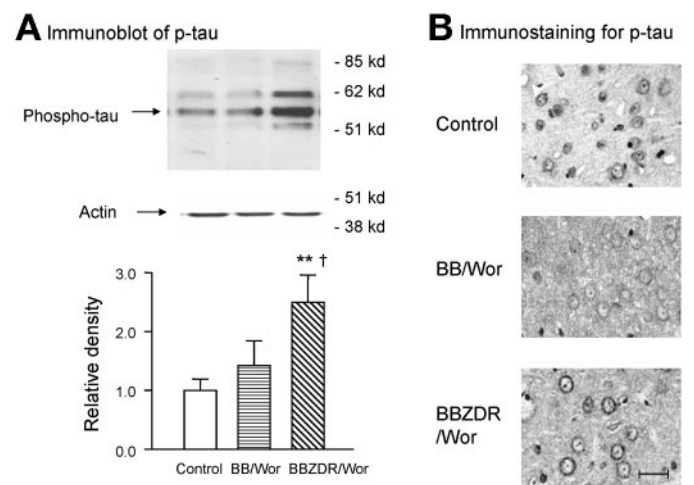


FIG. 4. Immunoblotting for phospho- $\tau$  (antibody PS-396) shows multiple bands representing phospho- $\tau$  isoforms, which were significantly ( $P < 0.01$ ) increased in the type 2 BBZDR/Wor rat (A). The expression in type 1 BB/Wor rats was not significantly increased (A). This corresponded to a stronger immunostainability in neuronal perikarya of layers II-III in type 2 diabetic rats, which was less evident in type 1 diabetic rats (B). Note an increased punctuate stainability of the neuropil in diabetic rats possibly corresponding to increased phospho- $\tau$  in neurites. The bar corresponds 50  $\mu$ m. \*\* $P < 0.01$  vs. control rats; † $P < 0.05$  vs. BB/Wor rats.

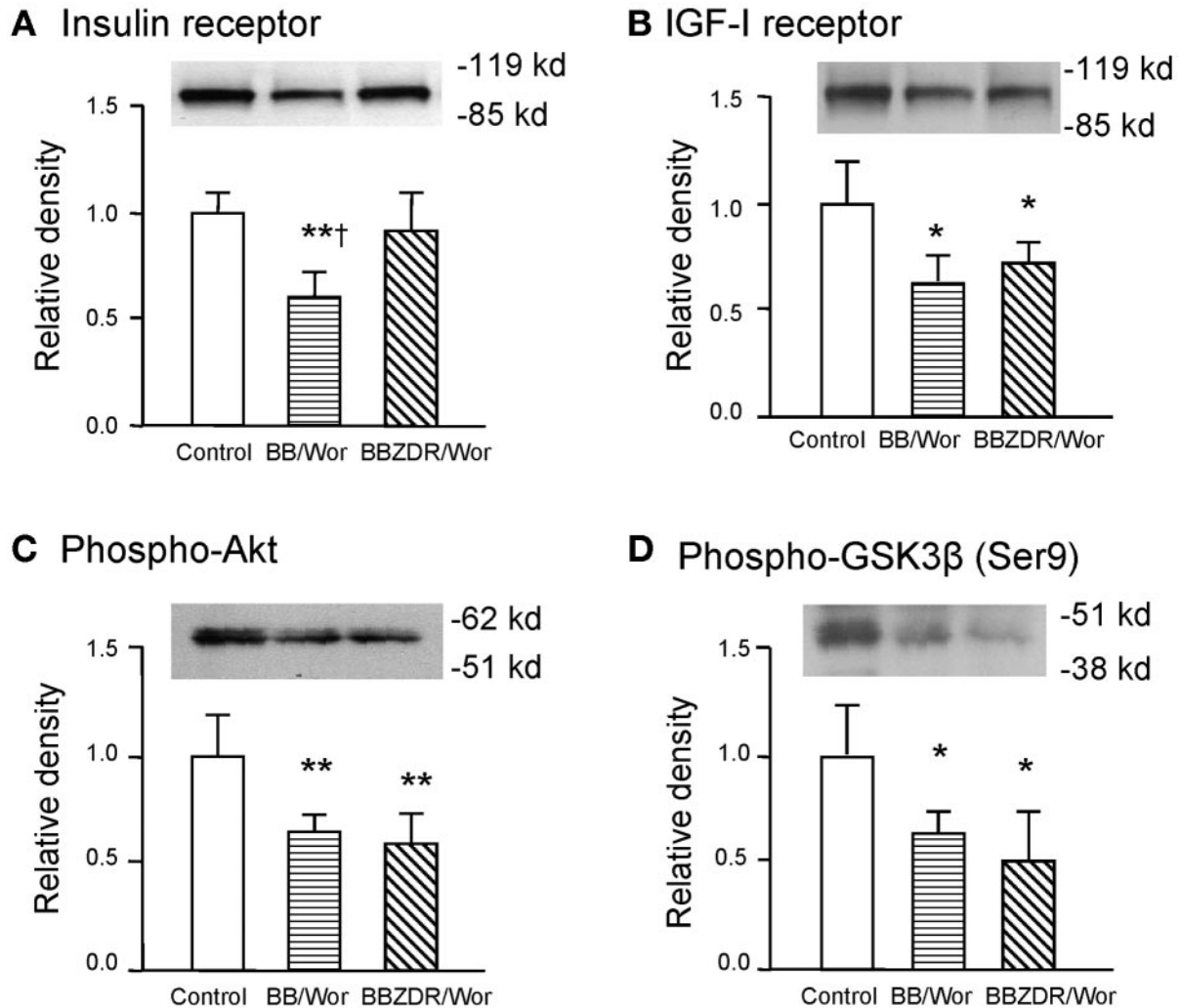


FIG. 5. The expression of insulin resistance was decreased in frontal cortex of type 1 but not in that of type 2 diabetic rats (A). IGF-1 receptor expression on the other hand was equally decreased in both diabetic models (B) as were the signal intermediaries phospho-Akt (C) and phosphorylated GSK-3 $\beta$  (Ser 9) (D). \* $P < 0.05$ , \*\* $P < 0.01$  vs. control rats; † $P < 0.05$  vs. BBZDR/Wor rats.

to the extracellular compartment (45,46), which would be consistent with the present findings of increased expression of soluble APP in BBZDR/Wor rats but not in BB/Wor rats. The abnormal APP metabolism in the type 1 diabetic BB/Wor rat could possibly be related to hyperglycemia and impaired cerebral blood flow (9), with elevated expression of inflammatory mediators such as cytokine transforming growth factor- $\beta$ 1 and interleukin-1 $\beta$ , which promote amyloidogenicity (47).

Activation of several caspases by  $\beta$ -amyloid has been linked to the cleavage of  $\tau$ , hence linking amyloid deposition and neurofibrillary tangles in Alzheimer's disease (48). We have previously demonstrated significant apoptotic stresses affecting hippocampal neurons in the same diabetic models (33). Isoforms of the  $\tau$  protein are highly susceptible to phosphorylation by several serine/threonine kinases such as mitogen-activated protein kinase, cdk5, and GSK-3 $\beta$  (32,34, 47,48), of which the latter appears to play a prominent role (28,32,48,49). GSK-3 $\beta$  (Ser 9) is phosphorylated in response to insulin and IGF via phospho-Akt downstream in the phosphatidylinositol 3 kinase pathway and inhibits GSK-3 $\beta$ . Here we demonstrated impaired phospho-Akt and GSK-3 $\beta$  (Ser 9), indirectly suggesting disinhibition of GSK-3 $\beta$ , which is a prime candidate for hyperphosphorylation of cleaved  $\tau$  (28,34,49,50), as demonstrated here in type 2 diabetic rats.

However, the relative absence of phospho- $\tau$  in type 1 diabetic rats suggest that additional  $\tau$ -kinases or other factors are operable in type 2 diabetic rats (33,35), since the suppression of phosphoAkt and GSK-3 $\beta$  (Ser 9) was similar in the two models. These possibilities are now actively being pursued in our laboratory.

In summary, this study has demonstrated neuronal loss, neurite degeneration accompanied by perturbations of APP metabolism, hyperphosphorylation of  $\tau$  isoforms, and impaired signaling of insulin and IGF-1 in two models of diabetes. The changes were more severe in the type 2 model and mirror those characterizing Alzheimer's disease. Although several potential underlying mechanisms remain to be explored, particularly the role of hypercholesterolemia and caveolin signaling, the present study suggests that mechanistic linkages do exist between spontaneous onset of experimental diabetes and Alzheimer's disease-like changes. We conclude that particularly type 2 experimental diabetes replicates the main abnormalities in Alzheimer's disease, such as abnormal amyloid handling, hyperphosphorylation of  $\tau$ , neurite degeneration, and neuronal loss.

#### ACKNOWLEDGMENTS

This research was supported in part by the Thomas Foundation, Bloomfield Hills, Michigan (to A.A.F.S.); the

Juvenile Diabetes Research Foundation, New York, New York (to A.A.F.S.), and the Morris Hood Diabetes Center, Detroit, Michigan (to Z.-G.L.).

## REFERENCES

- Kramer L, Fasching P, Madl C, Schneider B, Damjancic P, Waldhäusl W, Irisigier K, Grimm G: Previous episodes of hypoglycemic coma are not associated with permanent cognitive brain dysfunction in IDDM patients on intensive insulin treatment. *Diabetes* 47:1909–1914, 1998
- Ott A, Stolk RP, van Harskamp F, Pols HA, Hofman A, Breteler MM: Diabetes mellitus and the risk of dementia: the Rotterdam study. *Neurology* 58:1937–1941, 1999
- Arvanitakis Z, Wilson RS, Bievas JL, Evans DA, Bennett DA: Diabetes mellitus and risk of Alzheimer's disease and decline in cognitive function. *Arch Neurol* 61:661–666, 2004
- Sima AAF, Kamiya H, Li ZG: Insulin, C-peptide hyperglycemia and central nervous system complications in diabetes. *Eur J Pharmacol* 490:187–197, 2004
- Biessels GK, Kamel A, Urban LJ, Spruijt BM, Erkelens DW, Gispen WH: Water maze learning and hippocampal synaptic plasticity in streptozotocin-diabetic rats: effects of insulin treatment. *Brain Res* 800:125–135, 1998
- Li ZG, Zhang W, Grunberger G, Sima AAF: Hippocampal neuronal apoptosis in type 1 diabetes. *Brain Res* 946:212–231, 2002
- Sima AAF, Li ZG: The effect of C-peptide on cognitive dysfunction and hippocampal apoptosis in type 1 diabetes. *Diabetes* 54:1497–1505, 2005
- Hoyer S: Glucose metabolism and insulin receptor signal transduction in Alzheimer disease. *Eur J Pharmacol* 490:115–125, 2004
- Lin B, Ginsberg MD, Busto R: Hyperglycemic but not normoglycemic global ischemia induces marked early intraneuronal expression of  $\beta$ -amyloid precursor protein. *Brain Res* 888:107–116, 2001
- Caro E, Torres-Aleman I: The role of insulin and insulin-like growth factor I in the molecular and cellular mechanisms underlying the pathology of Alzheimer's disease. *Eur J Pharmacol* 490:127–133, 2004
- Banks WA, Jaspan JB, Kastin AJ: Effect of diabetes mellitus on the permeability of the blood-brain barrier to insulin. *Peptides* 18:1577–1584, 1997
- Busiguina S, Fernandez AM, Basrios V, Clark R, Tolbert DL, Berciano J, Torres-Aleman I: Neurodegeneration is associated with changes in serum insulin-like growth factors. *Neurobiol Dis* 7:657–665, 2000
- Gasparini L, Gouras GK, Wang R, Gross RS, Beal MF, Greengard P, Xu H: Stimulation of beta-amyloid precursor protein trafficking by insulin reduces intra-neuronal beta-amyloid and requires mitogen-activated protein kinase signaling. *J Neurosci* 21:2561–2570, 2001
- Steen E, Terry BM, Rivera EJ, Cannon JL, Neely TR, Tavares R, Xu XJ, Wands JR, de la Monte SM: Impaired insulin and insulin-like growth factor expression and signaling mechanisms in Alzheimer's disease: is this type 3 diabetes? *J Alzheimer's Dis* 7:63–80, 2005
- Roczeki A, Pellegrini S, Siciliano G, Murri L: Causative and susceptibility genes for Alzheimer's disease: a review. *Brain Res Bull* 61:1–24, 2003
- Blennow K, Skoog I: Genetic testing for Alzheimer's disease: how close is reality? *Curr Opin Psychiatry* 12:487–493, 1999
- Qui C, Winblad B, Viitanen M, Fratiglioni L: Pulse pressure and risk of Alzheimer's disease in persons aged 75 and older: a community-based longitudinal study. *Stroke* 34:594–599, 2003
- Kivipelto M, Helkala EL, Laakso MP, Hanninen T, Hallikainen M, Alhainen K, Soininen H, Tuomilehto J, Nissinen A: Midlife vascular risk factors and Alzheimer's disease in later life: longitudinal population-based study. *Br Med J* 322:1447–1451, 2001
- Selkoe DJ: Clearing the brain's amyloid cobweb. *Neuron* 32:177–180, 2001
- Zhang Y, McLaughlin R, Goodyer C, Le Blanc A: Selective cytotoxicity of intracellular amyloid  $\beta$  peptide 1–42 through p53 and Bax in cultured primary human neurons. *J Cell Biol* 156:519–529, 2002
- Sima AAF, D'Amato C: Dementias and other neurodegenerative diseases. In *Neuropathology: The Diagnostic Approach*. Garcia J, McKeever P, Sima AAF, Eds. Philadelphia, Mosby & Co., 1997, p. 581–636
- Spillantini MG, Goedert M: Tau protein pathology in neurodegenerative diseases. *Trends Neurosci* 21:428–433, 1998
- Sima AAF, Zhang W, Xu G, Sugimoto K, Guberski D, Yorek MA: A comparison of diabetic polyneuropathy in type-2 diabetic BBZDR/Wor-rat and in type 1 diabetic BB/Wor-rat. *Diabetologia* 43:786–793, 2000
- Sima AAF, Merry AC, Hall DE, Grant M, Murray FT: Guberski D: The BB/ZDR-rat: a model for type II diabetic neuropathy. *Exp Clin Endocrin Diab* 105:63–64, 1997
- Praxinos G, Watson C: *The Rat Brain in Stereotaxic Coordinates*. Sydney, Academic Press, 1982
- Eichmüller S, Stevenson PA, Paus R: A new method for double immunolabelling with primary antibodies from identical species. *J Immunol Methods* 190:225–265, 1996
- Hierck BP, Iperen LV, Gittenberger-deGroot AC, Poelman RE: Modified direct immunodetection allows study of murine tissue with mouse monoclonal antibodies. *J Histochem Cytochem* 42:1499–1502, 1994
- Lovestone S, Hartley CL, Pearce J, Anderton BH: Phosphorylation of tau by glycogen synthase-3 $\beta$  in intact mammalian cells: the effects on the organization and stability of microtubules. *Neurosci* 73:1145–1157, 1996
- Cohen AW, Combs TP, Scherer PE, Lisanti MP: Role of caveolin and caveolae in insulin signaling and diabetes. *Am J Physiol Endocrinol Metab* 28:E1151–E1160, 2003
- Nyström FH, Chen H, Long LN, Li Y, Quon MJ: Caveolin-1 interacts with the insulin receptor and can differentially modulate insulin signaling in transfected Coc-7 cells and rat adipose cells. *Mol Endocrinol* 13:2013–2024, 1999
- Ho L, Qin W, Pompl PN, Xiang Z, Wang J, Zhao Z, Peng Y, Cambareri G, Rocher A, Mobbs CV, Hof PR, Pasinetti GM: Diet-induced insulin resistance promotes amyloidosis in a transgenic mouse model of Alzheimer's disease. *FASEB J* 18:902–904, 2004
- Salkovic-Petrisic M, Tribl F, Schmidt M, Hoyer S, Riedeser P: Alzheimer-like changes in protein kinase B and glycogen synthase kinase-3 in rat frontal cortex and hippocampus after damage to the insulin signalling pathway. *J Neurochem* 96:1005–1015, 2005
- Li ZG, Zhang W, Sima AAF: The role of impaired insulin/IGF action in primary diabetic encephalopathy. *Brain Res* 1037:12–24, 2005
- Lambourne SL, Sellers LA, Bush TG, Choudhury SK, Emson PC, Suh YH, Wilkinson LS: Increased tau phosphorylation of mitogen-activated protein kinase consensus sites and cognitive decline in transgenic models for Alzheimer's disease and FTDP-17: evidence for distinct molecular processes underlying tau abnormalities. *Mol Cell Biol* 25:278–293, 2005
- Liu F, Iqbal K, Gnadke-Iqbal I, Hart GW, Gong CX: O-GlcNAcylation regulates phosphorylation of tau: a mechanism involved in Alzheimer's disease. *Proc Natl Acad Sci U S A* 101:10804–10809, 2004
- Sima AAF, Zhang W, Li ZG, Murakawa Y, Pierson CR: Molecular alterations underlie nodal and paranodal degeneration in type 1 diabetic neuropathy and are prevented by C-peptide. *Diabetes* 53:1556–1563, 2004
- Gustafson D, Rothenberg E, Blennow K, Stern B, Skoog I: An 18-year follow-up of overweight and risk of Alzheimer's disease. *Arch Intern Med* 163:1524–1528, 2003
- Pedersen WA, Flynn ER: Insulin resistance contributes to aberrant stress responses in the Tg2576 mouse model of Alzheimer's disease. *Neurobiol Dis* 17:500–506, 2004
- Patel NV, Gordon MN, Connor KE, Good RA, Engelman RW, Mason J, Morgan DG, Morgan TE, Finch CE: Caloric restriction attenuates A $\beta$ -deposition in Alzheimer transgenic models. *Neurobiol Aging* 26:995–1000, 2005
- Wang J, Ho L, Qin W, Rocher AB, Seror H, Humala N, Mania K, Dolios G, Wang R, Hof PR, Pasinetti GM: Caloric restriction attenuates  $\beta$ -amyloid neuropathology in a mouse model of Alzheimer's disease. *FASEB J* 19:659–661, 2005
- Haley RW: Is there a connection between concentration of cholesterol circulating in plasma and the rate of neurite plaques formation in Alzheimer's disease? *Arch Neurol* 57:1410–1412, 2000
- Kimura A, Mora S, Shigematsu S, Pessin JE, Saltiel AR: The insulin receptor catalyzes the tyrosine phosphorylation of caveolin-1. *J Biol Chem* 277:30153–30158, 2002
- Riddell DR, Christie G, Hussain I, Dingwall C: Compartmentalization of beta-secretase (Asp2) into low-buoyant density, noncaveolar lipid rafts. *Curr Biol* 11:1288–1293, 2001
- Ghribi O, Larsen B, Schrag M, Herman MM: High cholesterol content in neurons increases BACE, beta-amyloid, and phosphorylated tau levels in rabbit hippocampus. *Exp Neurol* 200:460–467, 2006
- Solano DC, Sironi M, Bonfini C, Solerte SB, Govoni S, Racchi M: Insulin regulates soluble amyloid precursor protein release via phosphatidylinositol-kinase dependent pathway. *FASEB J* 14:1015–1022, 2000
- Petanceska SS, Gaundy S: The phosphatidylinositol 3-kinase inhibitor Wortmannin alters the metabolism of the Alzheimer's amyloid precursor protein. *J Neurochem* 73:2316–2320, 1999
- Gray CW, Patel AJ: Regulation of  $\beta$ -amyloid precursor protein isoform mRNA's by transforming growth factor- $\beta$ 1 and interleukin- $\beta$ 1 in astrocytes. *Mol Brain Res* 19:251–256, 1993
- Gamblin TC, Chen F, Zambrano A, Abraha A, Lagalwar S, Guillozet AL, Lu M, Fu Y, Garcia-Sierra F, LaPointe N, Miller R, Berry RW, Binder LI, Cryns VL: Caspase cleavage of tau: linking amyloid and neurofibrillary tangles in Alzheimer's disease. *Proc Natl Acad Sci U S A* 100:10032–10037, 2003
- Hong M, Lee VM: Insulin and insulin-like growth factor-1 regulate tau phosphorylation in cultured human neurons. *J Biol Chem* 272:19547–19553, 1997
- Cho JH, Johnson GV: Glucocorticoid synthase kinase 3 $\beta$  induces caspase-cleaved tau aggregation in situ. *J Biol Chem* 279:54716–54723, 2004